

Low-Energy Hadron Production Data and Current Status of CERN Measurements*

Giles Barr^a and Ralph Engel^b

^aUniversity of Oxford, Department of Physics,
Denys Wilkinson Building, Keble Road, Oxford, OX1 3RH, United Kingdom

^bForschungszentrum Karlsruhe, Institut für Kernphysik, 76021 Karlsruhe, Germany

Data on low-energy hadron production in collisions of nucleons, pions and kaons with light nuclei are needed for many astrophysical and accelerator applications. Modern simulations have reached a level of accuracy that the lack of detailed understanding of hadron production processes has become one of the most important limitations to further improvements. After giving some examples of hadroproduction processes in astrophysics and neutrino experiments we briefly review existing fixed-target data on light nuclei. Preliminary results and prospects of current CERN measurements (HARP, NA49) are discussed.

Introduction

The increase in computational power in recent decades has allowed some very precise experimental measurements to be made. In particle physics, detector effects have been simulated using the Monte Carlo technique to the sub-percent level to obtain accurate corrections to measurements. Effects such as particle decay dynamics, electromagnetic shower propagation and energy loss are understood to a sufficient accuracy to allow these precise corrections to be determined. The interactions of hadrons, on the other hand reveal a considerable gap between the accuracy available in simulation programs and what is desired for certain applications. The reason for this is because the underlying theory of the strong interaction, Quantum Chromodynamics (QCD), is computationally difficult except for processes with large momentum transfer where perturbation theory can be applied.

The authors of simulation programs for hadron interactions have adopted either an empirical approach (insert tables and parametrizations of accelerator data into the computer code, for example, [1,2]) or a semi-empirical approach (design models which are motivated from a theoretical

point of view and then use accelerator data to tune the free parameters in the model to make the simulation fit the data, for example, [3,4]). These procedures both suffer from a lack of available hadron production data. As described below, good data is only available in a small fraction of the kinematically allowed and physically important region and for a small sample of target nuclei. Model builders are frequently faced with a choice in how to perform the extrapolation into uncharted parts of the phase space.

This article begins by describing some applications drawn from both cosmic ray physics and neutrino physics where more accurate simulations of hadron production would considerably improve the interpretation of existing data in terms of fundamental parameters or observables. We continue with a review of the current state of hadron production measurements; the authors' brief was to cover CERN experiments, although other experiments are also mentioned.

Muon production in extensive air showers

Extensive air showers (EAS) are produced by high energy cosmic rays colliding with air nuclei in the upper atmosphere. The accurate simulation of the resulting cascades may be used to predict the response (e.g. the distribution of muons on the Earth's surface). These simulations can

*Based on a talk given at the XIII International Symposium on Very High Energy Cosmic Ray Interactions, Pylos, Greece, 6-12 Sep 2004.

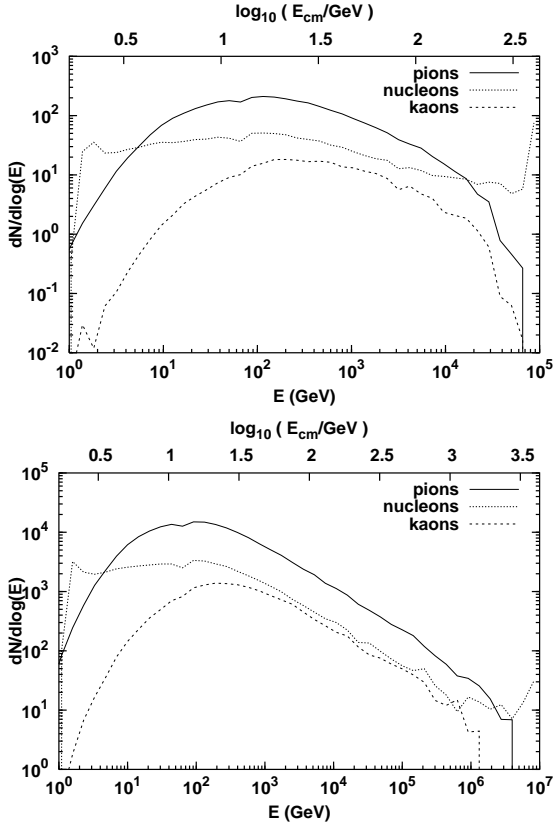


Figure 1. Energies and initiating particle type of interactions which lead to muon production in showers of $E_0 = 10^{14}$ eV (top) and $E_0 = 10^{16}$ eV (bottom). The upper horizontal axes show the equivalent hadron-nucleon c.m. energy.

then be used as a detector calibration; to deduce the characteristics of the original cosmic rays (e.g. the primary energy) based on the measurements in a detector. While the original cosmic ray might be of an energy which exceeds by far the energy available in accelerator based experiments, the showers contain a considerable number of lower energy interactions. The number of muons in EAS at detector level, often used together with the number of electrons to determine the primary energy and particle type of the shower, is partic-

ularly sensitive to hadron production processes in the energy range from a few tens of GeV to several TeV [5].

Figure 1 shows the energy distribution of those hadronic interactions in EAS that produce observable muons. For each muon arriving at detector level (1032 g/cm^2) with an energy $E_\mu > 250 \text{ MeV}$, one entry is made at the energy of hadron h_{GM}

$$h_{GM} + \text{air} \rightarrow h_M + X; \quad h_M \rightarrow \mu + X', \quad (1)$$

where h_{GM} and h_M can be considered as the muon's grandmother and mother particles, respectively. The simulations are done with CORSIKA [6] using QGSJET [7] as high-energy hadronic interaction model and GHEISHA [1] for interactions below 80 GeV. The curves illustrate the relative importance of different hadron interactions at various energies. Due to the competition between interaction and decay processes, the most probable energy is always between 100 to 200 GeV for charged pions and somewhat higher for charged kaons, almost independent of the primary EAS energy. This energy range of interactions relevant to low-energy muon production in EAS is in the reach of fixed-target accelerator experiments. Uncertainties in the prediction of muon numbers due to modeling of low-energy interactions are presented in Refs. [8,9]. The uncertainties increase with lateral distance from the shower core and exceed, for example, 20% at 2 km distance and 10^{19} eV. Therefore, a considerable gain in the quality of EAS simulations can be expected with new hadron production measurements.

Neutrino production in the atmosphere

Atmospheric neutrinos have become an exciting study as the Earth, it turns out, is just about the most convenient size to see neutrino oscillations [10] by comparing the zenith angle and energy distributions with calculations (for a review, see [11]). Even with an unsophisticated calculation, it is clear that a deficit of upward going muon neutrinos exists which is interpreted as the oscillation of $\nu_\mu \rightarrow \nu_\tau$.

Cosmic rays with energies extending down from EAS energies to a few GeV collide with the at-

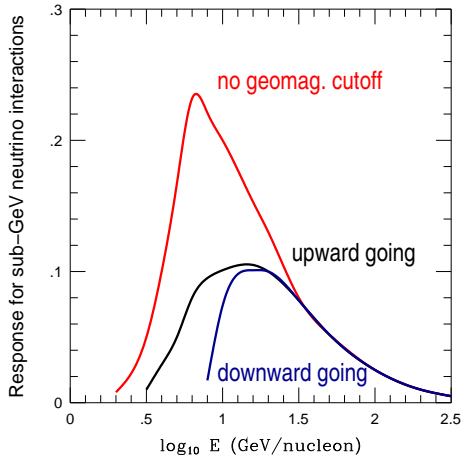


Figure 2. Response for sub-GeV muon-like events in SuperKamiokande to the energy of the primary cosmic ray nucleons (from [12]). Shown are simulations for solar minimum and no geomagnetic cutoff, events from lower hemisphere (upward going leptons), and events from upper hemisphere (downward going leptons).

mosphere. Neutrinos are produced in the decay of muons, pions and kaons in the resulting cascades. The neutrinos which are observed as contained events in underground detectors ($E_\nu \sim 1$ GeV) are produced mostly by the decay of pions from primaries in the range 2–200 GeV, see Fig 2. Higher energy neutrinos can be observed as upward going muons crossing the detector and are produced by primaries with energies up to ~ 10 TeV. At these higher energies, kaon production becomes extremely important due to their shorter lifetime than pions (which makes them more likely to decay than interact). Additionally, the energy available in the center of mass is much larger for $K \rightarrow \mu\nu$ than for $\pi \rightarrow \mu\nu$ and the steeply falling cosmic ray spectrum increases the importance of these kaon decays. With the recent improvements in primary flux measurements, the lack of comprehensive hadron production measurements over a more extensive fraction of the phase space is currently dominating the uncer-

tainty of the atmospheric neutrino fluxes.

Accelerator neutrino beams

Accelerator neutrino experiments have been used to extensively study the interactions of neutrinos including the discovery of neutral currents, precision electroweak measurements and the search and study of oscillations. The accelerator beams are produced in a similar way to the atmospheric neutrinos described above. Protons from the accelerator hit a target producing pions. The neutrinos produced in the decay of the pions (mostly ν_μ) are used for the experiment and the beam is stopped before many of the muons can decay. The neutrinos which are produced have a broad energy spectrum and are mostly ν_μ however there is a contamination of ν_e , $\bar{\nu}_\mu$ and $\bar{\nu}_e$ from muon and kaon decay. Precision measurements rely on an accurate knowledge of the neutrino energy spectrum and this is obtained from simulation with similar limitations from hadron production as for the applications described above. Many of the hadron production experiments have been performed by neutrino physicists with a specific goal of understanding their neutrino beam. For a review, see Ref. [13].

A radical new way of producing very intense accelerator neutrinos has been proposed (a neutrino factory) in which a beam is first produced in the way described above from a low (~ 2 – 10 GeV) energy proton beam. After the pions have been allowed to decay, the muons are collected and then inserted into a further accelerator where they are accelerated to energies $E_\mu \sim 50$ GeV. These muons are then circulated in a storage ring with long straight sections pointing towards several detector sites. The decay of the muons in the straight sections produces an intense source of neutrinos of known composition and spectrum. The gain in the concept is that power is applied by the accelerator directly to the muons. There are many difficulties to overcome, such as the construction of the target region, and the method of inserting the muons into the accelerator. It is possible in the further future that the concept may permit a muon collider to be constructed. One of the purposes of the HARP experiment, to be described below, is to investigate the hadron pro-

duction in order to optimize the efficiency of a neutrino factory target.

To summarize, there is considerable interest in the improvement of hadron production models for many applications.

Currently available data

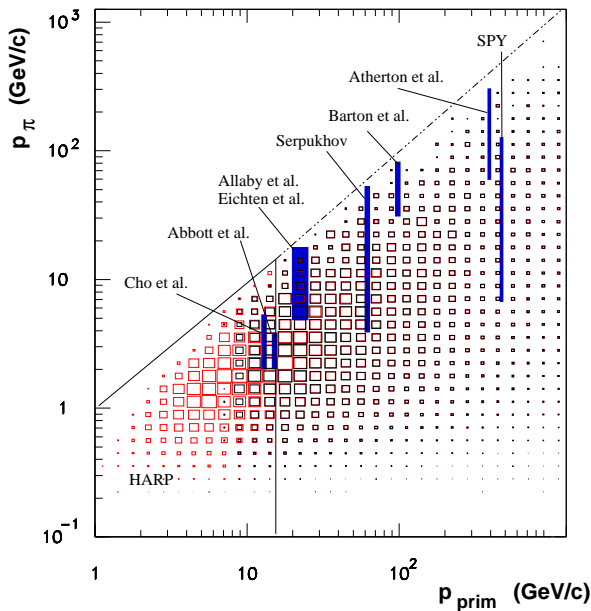


Figure 3. Summary of existing measurements of hadron production as a function of primary momentum p_{prim} and secondary pion momentum p_{π} . The black (red) boxes indicate the importance of each phase space region for downward (upward) atmospheric neutrino flux at SuperKamiokande. The difference is due to the Earth’s magnetic field. The vertical bars indicate where experimental data exist on low- A nuclei. The indicated measurements are Abbott et al. [14], Cho et al. [15], Eichten et al. [16], Allaby et al. [17], Barton et al. [18], Serpukhov [19], Atherton et al. [20], and SPY [21].

Figure 3 shows the current status of hadron production measurements for proton projectiles

in the region below 1 TeV primary energy. The vertical lines indicate the locations as a function of primary energy E_p and secondary energy E where *some* measurements have been made. An additional degree of freedom, not indicated on the plot is the transverse momentum p_T of the secondary particles (the production is symmetric in the φ angle). For most of the applications described above, the total production as a function of E_p and E is of main interest (i.e. integrated over p_T). Given the limited number of data points this integration is ambiguous and depends on the functional form used for the extrapolation to unmeasured phase space regions (for example, see discussion in [22]).

Since the p_T distributions control the lateral extent of a shower, the functional form of the hadron yields as a function of p_T is also important for EAS simulations. Atmospheric neutrinos are only observed one at a time (i.e. the chance of detecting two neutrinos from the same cosmic ray are negligible), the form of the p_T distribution is therefore less important for atmospheric neutrinos, however it is important to have the yield integrated over the full region of p_T . Neutrino beams select and focus pions from specific regions of phase space and so p_T distributions are important here also.

Many of the measurements shown in figure 3 have been made using ‘single armed spectrometers’. These are devices where the secondary particles are measured with a string of magnets tuned to transmit particles of a given momentum at a time. Examples of experiments of this type are given in Refs. [16,20,21]. The experiments can be ‘ready made’ by using the magnets in a secondary beam at an accelerator center such as CERN as the measuring device. A big advantage of this technique is that precise particle identification tuned to the momentum which the spectrometer is being used can be made to separate π , K and p extremely well. The measurements are somewhat painstaking, since only one angle and momentum of the secondary particles can be measured at a time and this is the reason why these measurements do not yet cover sufficient points in phase space for building models of hadron production.

A second technique is to use an emulsion stack in an accelerator beam. These experiments are limited in statistics and particle identification, however they can measure the complete phase space region in one exposure. Bubble chamber experiments have also been used, e.g. [23].

The experiments described below aim to measure a large fraction of (or the complete) secondary phase space in one setting by using large acceptance detectors. This will allow complete p_T distributions to be obtained in large regions of E . The experiments are not quite so good at particle identification as the single-arm experiments.

HARP

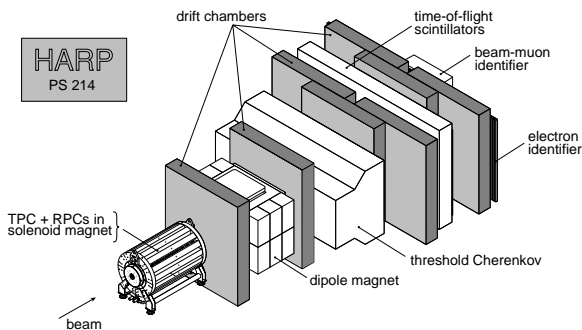


Figure 4. Layout of the HARP experiment [24, 25].

The HARP hadron production experiment [24] was built specifically to address the lack of coverage of phase space with good hadron production data for the applications as highlighted at the beginning of this article. A comprehensive range of targets (LH_2 , LD_2 , Be, C, LN_2 , LO_2 , Al, Cu, Sn, Ta, Pb, H_2O) of different atomic weights A and thickness have been exposed to beams from the CERN proton synchrotron (PS) with momenta between 1.5 and 15 GeV. Beams of both positive and negative targets have been used. Several replicas of neutrino beam targets have also been exposed. There are several solid targets with A

close to that of air and cryogenic (liquid) nitrogen and oxygen targets have also been exposed.

The beam is produced from a primary PS target at 24 GeV and the secondary particles are momentum selected and tagged with gas Cherenkov and time of flight detectors in the beam. All interactions are triggered and the type of beam particle determined offline; thereby, interactions with parent protons, kaons and pions are all available. The beam instrumentation also measures the trajectory of the incoming particle so that the impact position on the target can be reconstructed.

The detector is shown in figure 4. There are two distinct groups of detector to select different regions of phase space; large angle and small angle with respect to the beam direction.

The large angle detectors consist of a 80 cm diameter by 1.5 m long time projection chamber (TPC) enclosed in a 0.5 T solenoidal magnetic field. A hole in the center of the TPC allows the target to be inserted in the center of the sensitive region of the detector so that backward going particles can be measured. The TPC is the primary detection device for large angle tracks and pulse height information from the detector allows particle identification through ionization loss (dE/dx) measurement [26]. A layer of resistive plate detectors (RPCs) with ~ 160 ps resolution surrounds the detector for particle identification by time of flight [27]. The trigger is provided by a series of scintillating fiber detectors mounted along the central hole of the TPC.

The tracking detectors in the forward region (small angle) are drift chambers with three views (vertical and $\pm 5^\circ$). A vertical magnetic field bends the particles in the horizontal plane to determine the particle momentum. Downstream, a plane of scintillation counters with ~ 200 ps timing resolution is used to identify the particles by time of flight and provides 3σ π/p separation up to 4.5 GeV. A large (31 m^3) Cherenkov detector filled with C_4F_{10} provides good π/p separation at high momentum. Electron identification is provided by a scintillating fiber and lead sampling calorimeter.

The different phase space regions with the corresponding detector components employed for particle identification are shown in Fig. 5. The

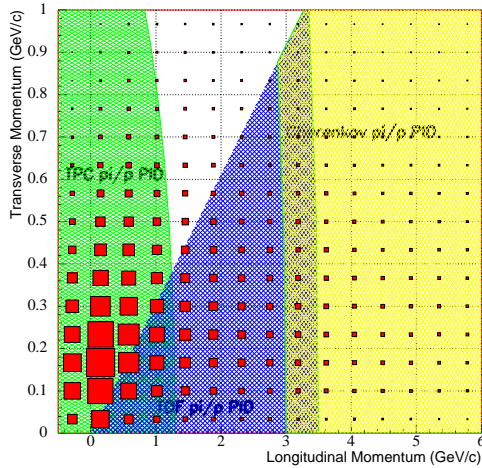


Figure 5. Secondary particle distribution in p-Be interactions at 15 GeV. Phase space regions for different methods of particle identification are superimposed.

squares show the expected secondary particle distribution for 15 GeV protons on Be.

Preliminary data on a thin 20 mm (5% of an interaction length) aluminium target, a short section of a replica target for the K2K experiment have become available recently [28]. Figure 6 shows the yield of secondary particles identified as pions as a function of both the momentum p and opening angle θ_z in the horizontal (bending) plane for momenta above 0.2 GeV/c. Fiducial cuts were applied at $25 < |\theta_z| < 200$ mrad and $|\theta_y| < 50$ mrad, where θ_y is the opening angle in the vertical plane.

NA49

The NA49 experiment [29] was first commissioned in 1994 and has been used since then with both lead ion and proton beams from the CERN SPS. The experiment is designed to cope with the extremely high multiplicity environment of a Pb-Pb collision at 400 GeV/Z.

NA49 is installed in the H2 beam line at the

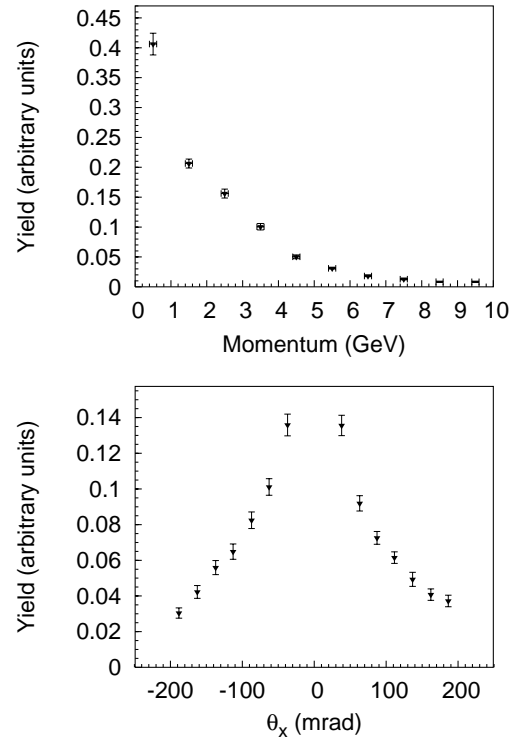


Figure 6. Recent HARP hadron production data on a thin aluminium target (K2K target replica) as a function of momentum and of angle in the horizontal plane [28].

CERN SPS. The experiment (Fig. 7) consists of two ($2\text{ m} \times 2.5\text{ m} \times 0.98\text{ m}$ overall dimensions) TPCs (VTPC1 and VTPC2) supported inside 1.7 T super-conducting magnets. Downstream, there are two further TPCs ($3.9\text{ m} \times 3.9\text{ m} \times 1.8\text{ m}$) (MTPCL and MTPCR) which measure the tracks once they emerge from the magnetic field. Approximately 100 samplings of the ionization loss are made per track in the combined TPCs to determine the particle identification from the relativistic rise section of the energy loss curves. This is the principle form of particle identification in the experiment. The target is mounted in front of the first TPC, so, unlike HARP, only forward

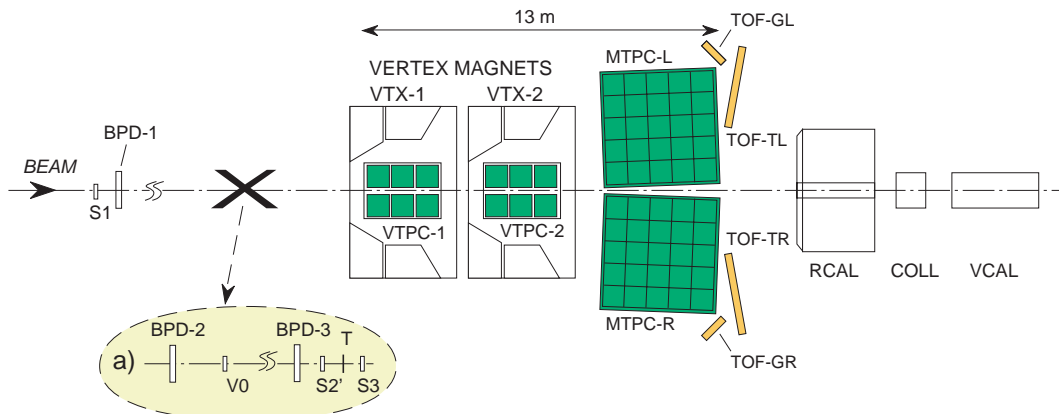


Figure 7. Plan layout of the NA49 experiment. The four TPCs are shown (VTPC1,2 with magnetic field and MTPC L,R). The position of the target is indicated by a 'T' in the inset a) immediately in front of VTPC1. Beam position detectors (BPD) and trigger counters S1,2,3 are also shown.

tracks may be measured. The detector has excellent acceptance for particles with $x_f > 0$. Particles with momenta above $80 \text{ GeV}/c$, pass through the gap between TPCs (essential for heavy ion running to avoid space charge from ionization from the uninteracted beam). A new thin gap-TPC was added to the experiment to allow track detection (but not particle ID) in this region.

A differential beam Cherenkov detector (two compartments, with pressures set appropriately to be just above and below the Cherenkov threshold of the desired particle) is used in the trigger so that only events which originated from protons are in the data sample. A beam particle tracking system (BPD) allows the impact position on the target to be known precisely.

The experiment has recently been run with a low-bias trigger with a carbon target for the purpose of measuring hadron production for atmospheric neutrinos. A one week run with protons at 158 GeV and 100 GeV has yielded a sample of data with over 500,000 tracks [30] and the analysis will be completed shortly.

The NA49 experiment has finished its data taking programme. Currently a new collaboration is forming to perform an extended series of mea-

surements [31], including hadron production measurements at CERN. The experiment will use the existing NA49 apparatus and it is intended to collect a considerably more extensive set of measurements than obtained in the pilot experiment described above. It is planned to perform a primary energy scan from 40 to about 200 GeV and a variety of projectiles will be studied including protons and light nuclei such as helium and carbon.

Summary

There are many reasons why the world's hadron production data is not enough. In particular series of many points in phase space are required to allow the functional form of hadron production measurements to be known precisely across all p_T and secondary particle momenta. Two new measurements at CERN, HARP (a purpose built experiment) and NA49 have been described. Data at both experiments have been collected and are currently being analyzed. Preliminary results from HARP have recently become available.

Additionally, there are new experiments in the USA which have, or soon will have hadron production data. The E910 experiment at Brookhaven [32] has data in the range $6\text{--}18 \text{ GeV}$

on beryllium [33,34] and the MIPP experiment (specifically built for hadron production measurements) at FNAL [35] has concluded its engineering run in 2004 and is scheduled to collect data in the primary energy range 5–120 GeV in 2005 [36].

Acknowledgements

The authors would like to thank members of both the HARP and NA49 collaborations for help in the preparation of this contribution and in particular G. Catanese and J. Panman for their help during preparation of the presentation. They would also like to thank T. Gaisser, S. Robbins, and T. Stanev for many useful discussions and help on simulation of cosmic rays. One of the authors, R.E., gratefully acknowledges the collaboration with A. Haungs, D. Heck, C. Meurer, and M. Roth on the importance of low-energy interactions in air showers.

REFERENCES

1. H. Fesefeldt: Report PITHA-85/02, RWTH Aachen, 1985.
2. R. Engel, G. Barr, T. K. Gaisser, S. Robbins and T. Stanev: Proc. of 28th ICRC, Tsukuba, Japan, (2003) 1603.
3. A. Fasso, A. Ferrari, J. Ranft and R. P. Sala: Proc. of MC2000, Lisbon, Portugal, (2001) 955.
4. M. Bleicher et al.: J. Phys. G: Nucl. Part. Phys. 25 (1999) 1859.
5. R. Engel, T. K. Gaisser and T. Stanev: Proc. of XXIX ISMD, Brown University, USA (2000) p. 457.
6. D. Heck, J. Knapp, J. Capdevielle, G. Schatz and T. Thouw: Wissenschaftliche Berichte FZKA 6019, Forschungszentrum Karlsruhe, 1998.
7. N. N. Kalmykov, S. Ostapchenko and A. I. Pavlov: Nucl. Phys. B (Proc. Suppl.) 52B (1997) 17.
8. H.-J. Drescher and G. R. Farrar: Astropart. Phys. 19 (2003) 235.
9. D. Heck et al.: Proc of 28th ICRC, Tsukuba, Japan, (2003) 279; D. Heck, these proceedings and astro-ph/0410735.
10. Super-Kamiokande: Y. Fukuda et al.: Phys. Rev. Lett. 81 (1998) 1562.
11. T. K. Gaisser and M. Honda: Ann. Rev. Nucl. Part. Sci. 52 (2002) 153.
12. T. K. Gaisser: Nucl. Phys. Proc. Suppl. 77 (1999) 133.
13. M. G. Catanese: talk presented at the 6th Intl. Workshop on Neutrino Factories and Superbeams (NuFact04) Osaka, July 2004.
14. T. Abbott et al.: Phys. Rev. D45 (1992) 3906.
15. Y. Cho et al.: Phys. Rev. D4 (1971) 1967.
16. T. Eichten et al.: Nucl. Phys. B44 (1972) 333.
17. J. V. Allaby et al.: CERN Yellow Report 70-12, 1970.
18. D. S. Barton et al.: Phys. Rev. D27 (1983) 2580.
19. N. I. Bozhko et al.: Sov. J. Nucl. Phys. 29(3) (1979) 347; Sov. J. Nucl. Phys. 31(5) (1980) 644; Sov. J. Nucl. Phys. 31(6) (1980) 775.
20. H. W. Atherton et al.: CERN-80-07, 1980.
21. SPY Collab.: G. Ambrosini et al.: Phys. Lett. B420 (1998) 225; Phys. Lett. B425 (1998) 208; Eur. Phys. J. C10 (1999) 605.
22. R. Engel, T. K. Gaisser and T. Stanev: Phys. Lett. B472 (2000) 113.
23. H. J. Mück et al.: Phys. Lett. B39 (1972) 303.
24. M. G. Catanese et al.: CERN-SPSC-99-35, 1999.
25. HARP Collab.: M. Ellis et al.: J. Phys. G29 (2003) 1613.
26. HARP Collab.: G. Prior et al.: Nucl. Phys. Proc. Suppl. 125 (2003) 37.
27. M. Bogomilov et al.: Nucl. Instrum. Meth. A508 (2003) 152.
28. HARP Collab.: I. Kato: talk presented at the 6th Intl. Workshop on Neutrino Factories and Superbeams (NuFact04) Osaka, July 2004.
29. NA49 Collab.: S. Afanasev et al.: Nucl. Instrum. Meth. A430 (1999) 210.
30. NA49 Collab.: G. Barr et al.: Proc. of 28th ICRC, Tsukuba, Japan, (2003) 1551.
31. NA49' Collab.: J. Bartke et al.: CERN-SPSC/2003-038 and SPSC-EOI-01, 2003.
32. <http://www.phy.bnl.gov/~e910/>
33. E910 Collab.: I. Chemakin et al.: Phys. Rev. D65 (2002) 024904.
34. E910 Collab.: J. Link et al.: talk presented at the 6th Intl. Workshop on Neutrino Factories and Superbeams (NuFact04) Osaka, July 2004.
35. <http://ppd.fnal.gov/experiments/e907/>
36. R. Raja: hep-ex/0501005.